Oxidoreduction potential controlling for increasing the fermentability of enzymatically hydrolyzed steam-exploded corn stover for butanol production

Min Wang (minw@tust.edu.cn)
Tianjin University of Science and Technology
Menglei Xia
Tianjin University of Science and Technology
Di Wang
Tianjin University of Science and Technology
Yiming Xia
Tianjin University of Science and Technology
Haijiao Shi
Tianjin University of Science and Technology
Zhongyu Tian
Tianjin University of Science and Technology
Yu Zheng
Tianjin University of Science and Technology

Research Article

Keywords: Clostridium acetobutylicum, Steam-exploded corn stover, Fermentability, Oxidoreduction potential controlling, Enhancement mechanism analysis

Posted Date: March 10th, 2022

DOI: https://doi.org/10.21203/rs.3.rs-1409943/v1

Abstract

Background: Lignocellulosic biomass is recognized as an effective potential substrate for biobutanol production. Though many pretreatment and detoxification methods have been set up, the fermentability of detoxicated lignocellulosic substrate is still far lower than that of starchy feedstocks. On the other hand, the number of recent efforts on rational metabolic engineering approaches to increase butanol production in *Clostridium* strains are also quite limited, demonstrating the physiological complexity of solventogenic clostridia. In fact, the strain performance is greatly impacted by process controlling. developing efficient process control strategies could be a feasible solution to this problem.

Result: In this study, oxidoreduction potential (ORP) controlling was applied to increase the fermentability of enzymatically hydrolyzed steam-exploded corn stover (SECS) for butanol production. When ORP of detoxicated SECS was controlled at -350mV, the period of fermentation was shortened by 6 h with an increase of 27.5% in the total solvent (to 18.1 g/L) and 34.2% in butanol (to 10.2 g/L) respectively. Silico modeling revealed that the fluxes of NADPH, NADH and ATP strongly differed between the different scenarios. Quantitative analysis showed that intracellular concentrations of ATP, NADPH/$NADP^+$ and NADH/NAD^+ were increased by 25.1%–81.8% and 62.5%. ORP controlling also resulted in a 2.1-fold increase in butyraldehyde dehydrogenase, a 1.2-fold increase in butanol dehydrogenase and 29% increase in the cell integrity.

Conclusion: ORP control strategy is effective for altering intracellular metabolic profiles and can significantly improve *Clostridium* cell growth and butanol production. The working mechanism can be summarized into three aspects: First, Glycolysis and TCA circulation pathway are strengthened through key nodes such as pyruvate carboxylase [EC: 6.4.1.1], which provides sufficient NADH and NADPH for the cell. Second, sufficient ATP is provided to avoid “acid crash”. Third, the key enzymes activities regulating butanol biosynthesis and cell membrane integrity was improved.

1. Introduction

Biobutanol may play a pivotal role in the overall success of the biofuels industry and is considered as a promising next generation liquid fuel because of its superior characteristics over ethanol (Wang & Chen, 2011). However, the high cost of conventional substrates (such as maize and molasses) forms one of the main bottlenecks for economic viability. Therefore, lignocellulosic biomass is recognized as an effective potential substrate for biobutanol production because of its abundance, renewability, and cost-effective characteristics (Chen & Qiu, 2010).

Plant biomass has evolved complex structural and chemical mechanisms for resisting assault on its structural sugars from the microbial and animal (Himmel et al., 2007). Hence, pretreatment and hydrolysis of lignocellulosic biomass before fermentation are essential to convert the complex structure of cellulose and hemicelluloses into simple sugars (Baral & Shah, 2014). During pretreatment, some fractions of cellulose and hemicellulose are converted into fermentable sugars, which can further be converted to acetone-butanol-ethanol (ABE). However, sugar and lignin degradation compounds including weak acids, furan derivatives, and phenolic compounds are also formed, which have severely inhibitory effects on the *Clostridium* (Ibraheem & Ndimba, 2013). They damage the cell membrane to maintain internal pH and makes it permeable to adenosine diphosphate and some ions, inhibits glucose uptake, and, subsequently, causes cell lysis (Bowles & Ellefson, 1985; Ibraheem & Ndimba, 2013). Over the past years, several detoxification protocols have been proposed and introduced, including physical (e.g. adsorption with activated carbon or ion exchange resins), chemical (e.g. lime or alkali treatment, ionic liquids; mixtures of cationic and anionic salts that melt mostly below 100°C) or biological (e.g. laccase or peroxidase) measures (Ibraheem & Ndimba, 2013). To date, most of the detoxification protocols are far from satisfactory (Ibraheem & Ndimba, 2013; Wang & Chen, 2011). And it is not feasible to remove all the inhibitors at the expense of high investment. It is of importance to explore new strategies for solving this urgent problem.

Redox potential, known as oxidation-reduction or oxidoreduction potential (ORP), reflects overall electron transfer and redox balance involved in intracellular metabolism. Many biological functions of cells are affected by ORP levels through gene expression and enzyme synthesis, which consequently affect signal sensing and transduction, and ultimately metabolic profiles, particularly under stress conditions associated with industrial production (Liu et al., 2013a). Since extracellular ORP that can be detected conveniently in fermentation broth by an ORP electrode synchronously reflects intracellular ORP status. So far ORP controlling strategies have been successfully developed and applied for altering intracellular ORP conditions and cell metabolism (Liu et al., 2013a; Wang et al., 2012). Vasconcelos et al. (1994) proved that changing the overall degree of reduction of the substrate, using mixtures of glucose and glycerol, generated significance on the enzymatic pattern of *C. acetobutylicum*. Wang et al. (2012) reported that the biphasic metabolism of *C. acetobutylicum* could be changed by ORP regulation. When using air to control the ORP of the fermentation broth at -290 mV, an earlier initiation of solventogenesis was achieved. Li et al. (2014) indicated that an increase in butanol/acetone ratio and NADH regeneration could be realized when enriching reductive environment of using cassava-based substrate. However, to data, it remains unclear whether ORP controlling can increase the fermentability of enzymatically hydrolyzed steam-exploded corn stover for butanol production (SECS) for butanol production yet.

The genome-scale metabolic (GSM) model analysis is a powerful tool for understanding the metabolic capacities of an organism and developing metabolic engineering strategies for strain development. By integrating all of the experimentally determined metabolic reactions taking place in an organism of interest, it can generate accurate predictions and informative hypotheses for cellular metabolism(Cheng et al., 2021; Rodenburg et al., 2021). It has been widely used in molecular mechanism study (Zhu et al., 2020), exogenous pathway designment (Zheng et al., 2017) and so on. Comparing with the traditional omics methodology, it let the researchers exactly calculate the generation and distribution of energy and electron-mediating organic cofactors NAD(P)H (Li et al., 2021a).

In this study, the effect of inhibitors on butanol biosynthesis was firstly investigated by comparing fermentation performance of detoxicated SECS and synthesized medium. Secondly, combined with the efficient detoxification method built previously (Wang & Chen, 2011), the effects of controlling the ORP on the fermentability of detoxicated SECS at different levels were studied. Lastly, the enhancement mechanism of ORP controlling was investigated using genome scale metabolic flux analysis, energy status detection, enzymes activity measurement and cell membrane integrity evaluation.

2. Methods

2.1 Steam explosion pretreatment

Corn stover was obtained from a local farm in Tianjin, China. Steam explosion pretreatment was carried out in a 7.5-L batch reactor as described in a previous work (Xia et al., 2020). About 200 g air-dried chipped corn stover was soaked in 200 mL distilled water for 15 min, fed into the reactor at 1.1 MPa for 4 min. After steam explosion, the material was washed with 1 L of 80 ^{o}C water and filtered by nylon cloth (200 meshes) and then dried at 65 ^{o}C until constant weight (< 3% of moisture content) for enzymatic hydrolysis.

2.2 Enzymatic hydrolysis and detoxification pretreatment

Enzymatic hydrolysis experiments were conducted with the method of Wang and Chen (2011). The hydrolysis reaction was conducted at 50 ^{o}C, with shaking at 150 rpm for 48 h. Then the hydrolysate was separated from the mixture by vacuum filtration, and concentrated in a rotary vacuum evaporator at 60 ^{o}C. The total sugar in the hydrolysate was about 60 g/L. The concentrated hydrolysate was treated with 7.5% (w/v) of granular activated charcoal at 30 ^{o}C with shaking at 150 rpm for 12 h. After that the activated charcoals were separated from hydrolysate by vacuum filtration and the hydrolysate was adjusted to pH 6.5 ± 0.5 using $Ca(OH)_2$.

2.3 Microorganism and culture conditions

The working strain *C. acetobutylicum* ATCC 824 was purchased from China General Microbiological Culture Collection Center and repetitively domesticated using the method of Yu et al (Liu et al., 2013b). Stock cultures were stored at -80 ^{o}C as 15% (v/v) glycerol stocks of cells, which were grown to an OD_{600} of 0.8-1.0. After being removed from the freezer, the strain was heat-shocked at 70 ^{o}C for 2 min, and then inoculated into a glass tube (diameter, 3 cm; 15 cm height) containing 25 mL of 7% (w/v) corn mash used as the see d medium, followed by an incubation period of 30 h at 37 ^{o}C. There are two kinds of fermentation medium used in our study: enzymatically hydrolyzed steam-exploded corn stover (SECS) medium and synthesized medium (SM). The components of detoxicated SECS were as following: concentrated hydrolysate, 6 g/L $(NH_4)_2SO_4$, 1.768 g/L KH_2PO_4, 2.938 g/L K_2HPO_4, 2 g/L $CaCO_3$, 10 mg/L *p*-aminobenzoic acid, and 10 mg/L biotin. The components of synthesis medium include 30 g/L glucose, 20 g/L xylose, 10 g/L cellose, 6 g/L $(NH_4)_2SO_4$, 1.768 g/L KH_2PO_4, 2.938 g/L K_2HPO_4, 2 g/L $CaCO_3$, 10 mg/L *p*-aminobenzoic acid, and 10 mg/L biotin. The synthesis medium was set as reference. In all experiments, the initial pH of the medium was adjusted to 6.5 with 1 M NaOH and heat sterilized at 115 ^{o}C for 30 min. Glucose was autoclaved separately and mixed in an anaerobic chamber. *p*- aminobenzoic acid was also added separately as a filter sterilized solution. Methyl viologen and rutin stock were sterilized by filtration and added into the all the medium to a final concentration of 200 μM and 490μM respectively. All chemicals used in this study were purchased from Beijing Chemicals Factory, Beijing, China. All the experiments were carried out in anaerobic incubator (YQX-II, Xinmiao, China), which was purged with 99.9% N_2 to ensure 100% anaerobic conditions during the whole process. The fermentation condition was described in our previous study (Xia et al., 2020) except the fermentation were carried out in 2 L flask with a working volume of 1 L.

2.4 Analytical procedures

Acetone-butanol-ethanol (ABE) and acids (acetate and butyrate) were measured with the methods of our previously employed (Xia et al., 2020). Glucose, xylose, cellobiose, furfural, and 5-hydroxymethylfurfural were determined by high-performance liquid chromatography (Agilent 1200 HPLC, Agilent Technologies, USA) with an Aminex HPX-87H column (300 mm × 7.8 mm, Bio-Rad Laboratories Inc.) and a refractive index detector. Soluble lignin was detected by ultraviolet spectra and estimated by the method of Mussatto and Roberto (2006). All the standards were purchased from Sigma-Aldrich (St. Louis, MO). To determine the dry cell weight, 10 mL culture sample was taken from the fermentation vessel and centrifuged at 2,500 × g for 3 min. Then, cells were washed with ice-cold phosphate-buffered saline (PBS) for five times and kept at 60 ^{o}C until the constant weight.

2.5 ORP detection and control strategy

The ORP controlling instrument is shown in Fig. 1. An ORP electrode (Pt4805-DPAS-SC-K85; Mettler-Toledo, Switzerland) was connected with ORP console (a relay) and peristaltic pumps. ORP level of the fermentation broth was controlled at the set value by pumping the sterilized air (to increase the ORP level) or though input of 30 g/L Na_2S (to decrease the ORP level). Before measurement, the electrode was calibrated with redox standard solution.

2.6 Genome scale metabolic flux analysis

The genome-scale model for *C. acetobutylicum* was adopted from the previously published model by Lee et al. (2008) and the full information was given in Appendix A. Briefly, the reconstructed metabolic network was represented in a mathematical format in a stoichiometric matrix S, where the rows correspond to the metabolites and columns correspond to the reactions in the network (Nagarajan et al., 2013). Flux balance analysis simulations were carried out using the COBRA Toolbox (Heirendt et al., 2019; Zheng et al., 2017). Because the *C. acetobutylicum* strain has two distinct phases of product formation: acidogenesis and solventogenesis, the objective function was set differently. Maximizing growth was used to calculate the flux distribution in the acidogenesis phase. Minimization of metabolic adjustment (MOMA) method proposed by Lee et al. (2008) was employed in the solventogenesis phase.

2.7 The measurement methods of enzyme activity

Preparation of cell extracts were carried out following the method of Vasconcelos et al. (1994). Butanol and butyraldehyde dehydrogenases (EC:1.1.1- and EC.1.2.1.10) were carried out by the method of except that substrate concentrations were as following: acetaldehyde, 20 mM, butyraldehyde, 11 mM; acetyl coenzyme A (acetyl-CoA), 0.5 mM; and butyryl-CoA, 0.5 mM. Phosphotransacetylase (EC 2.3.1.8) was essayed was descried by except that crude extract was used instead of dialyzed extract. The CoA liberated was determined with DTNB [5,5'-dithiobis (2-nitrobenzoic acid)] at 410 nm (ε_{410} = 13.8 mM^{-1} cm^{-1}).

2.8 Detection of cell membrane integrity

0.5 mL culture sample was taken from the fermentation vessel and centrifuged at 2,500 × g for 1 min. Then, cells were washed with 37 ^{o}C phosphate-buffered saline (PBS). After be washed for two times, cells were mixed with 0.5 mL of PBS containing 2.5 mg of fluorescein diacetate (FDA) and incubated for 10 min at 37 ^{o}C in the dark. Then, 0.3 of the pretreated broth was transferred into 96-well plate. The relative levels of fluorescence were quantified in fluorospectro-photometer (F-4600, Hitachi, Japan) at an excitation wavelength at 495 nm and an emission wavelength at 535 nm respectively.

2.9 Statistical analysis

All experiments were performed independently at least three times, and the average values with standard errors were reported. Statistical analysis was performed using the Student's t-test. P values of less than 0.05 were considered statistically significant.

3. Results And Discussion

3.1 Comparison of the fermentability between detoxicated SECS and starchy feedstocks for butanol production

As Table I shows, the main components of SECS are glucose (59.3%), xylose (23.4%) and cellulose (11.35%); during the pretreatment process, a complex mixture of microbial inhibitors is also generated, which are mainly soluble lignin (3.55 g/L), vanillin and ferulic acid together with other aromatic compounds (see Appendix B).

Figure 2 compares the fermentation performances of *C. acetobutylicum* ATCC 824 in SECS and synthetized medium (as reference). Based on our experiments, the order of sugar preference by *C. acetobutylicum* ATCC 824 can be summarized as glucose > xylose > cellulose. Due to inhibitors, strains showed low sugar utilization ability when in the SECS medium. The utilization rates of glucose, xylose and cellulose were 87.5%, 31.0% and 33.3% of those in synthetized medium respectively. As a result, cell growth was inhibited, which was only 65.7% of that in synthetized medium. Wang and Chen (2011) proved soluble lignin as the main fermentation inhibitors for *C. acetobutylicum* strains by supplementing inhibitors into the synthetized medium. It is because soluble lignin are phenolic compounds, which cause increase in membrane fluidity, a property known to affect membrane permeability (Heipieper et al., 1994) causing leakage of cellular contents or even cell death (Ezeji et al., 2007). There also shows significant difference on product profiles between the two groups: cells in SECS produced less alcohols (acetone, butanol and ethanol) but higher level of acids (butyrate and acetate), suggesting cell in SECS shifts metabolism to favor the biosynthesis of acids, such similar pattern was also found in our previous study (Xia et al., 2015a). A typical biphasic fermentation can be observed in synthetized medium: acetate and butyrate were accumulated mainly in the first 48 h; butyrate was then reused and solvents were produced rapidly with final production of butanol, acetone and ethanol of 12.1 g/L, 2.9 g/L and 4.1 g/L, respectively. Different from described above, instead of absorbed by cells for butanol biosynthesis (Ezeji et al., 2010), butyrate in SECS kept been produced during 48–96 h, resulting in lower final alcohol productions with 7.6 g/L butanol, 2.4g/L acetone and 3.0 g/L ethanol. The ORP profiles also showed significant difference: the ORP of SECS decreased rapidly from the initial − 80 mV to 170mV within 12 h (lag phase) and then gradually rose to 157 mV until the end of the fermentation. As a contrast, the ORP in the synthesized medium decreased to -360 mV at 36 h and kept relatively stable during the fermentation process (36–72 h), and then increased to -220 mV during the following phase. It thus can be concluded that the fermentability of detoxificated SECS is still far lower than that of starchy stocks. The tiny inhibitors remained can still inhibit the metabolism behaviors of *C. acetobutylicum* ATCC 824 during the butanol fermentation.

3.2 Enhancement of the fermentability of detoxificated SECS by ORP controlling

To enhance the fermentability of detoxificated SECS, ORP controlling strategy was designed and carried out. The fermentation performances under different controlling strategies were summarized in Table 2 and Fig. 3 (The fermentation profiles under ORP controlling which started at 0 h were given in Appendix C).

Table 1
Components of enzymatically hydrolyzed steam-exploded corn stover

Materials	Concentration (g/L)
Total sugar	63.75
Glucose	37.83
Xylose	14.92
Cellobiose	7.24
Acetic Acid	0.16
Furfural	0.046
5- hydroxymethyl furfural	0.011
Soluble lignin	3.55
Other components*	< 0. 1
* See Supplementary II.	

Table 2
Comparison of cell growth and the yield of acetone, butanol and ethanol using different ORP controlling strategies

ORP value	Starting time for controlling	Fermentation time (h)	End product formed (g/L)					Final Biomass (g/L)	Sugar consumed (%)		
			Ethanol	Acetate	Butanol	Butyrate	Acetone		glucose	xylose	cellobiose
Uncontrolled		**96 h**	**4.2**	**7.2**	**7.6**	**4.1**	**2.4**	**3.1**	94.3	80.2	81.5
-250	0 h	96 h	1.6	2.7	3.2	2.9	0.9	1.7	40.3	30.6	34.1
-300	0 h	96 h	2.4	3.7	4.1	2.7	1.4	2.2	74.9	50.3	50.4
-350	0 h	96h	2.2	4.1	3.2	3.1	2.6	2.5	84.1	64.3	55.8
-400	0 h	96h	0.9	1.9	2.6	1.7	1.1	1.8	31.4	26.4	22.1
-250	24 h	96 h	3.1	5.0	4.4	4.9	2.8	2.8	87.4	80.7	79.7
-275	24 h	90 h	5.1	5.4	7.6	3.7	2.6	3.4	96.4	84.4	80.6
-300	24 h	90 h	5.6	4.2	8.8	3.5	3.1	3.8	97.2	84.2	82.1
-350	24 h	90 h	5.9	3.9	10.2	2.7	2.0	4.6	98.7	86.5	88.1
-400	24 h	96 h	1.7	3.1	3.7	2.3	0.4	2.9	86.4	76.4	70.4

When the ORP controlling was started at the first 24 h, cell growth was even worse than the ORP uncontrolled fermentation, indicating the optimal ORP in lag phase (0 ~ 24 h) was not a stable value. (Unless specially indicated, the discussion below refers to the ORP controlling which started at 24 h). Within the range of -270 ~ -350 mV, cell growth and sugar utilization increased with the decease of ORP. At ORP of -270 mV, -300mV and − 350mV, the biomass was increased by 9.6%, 22.5% and 38.7% comparing with the uncontrolled group. Glucose utilization rate at ORP of -270 mV, -300mV and − 350mV was 96.4%, 97.2% and 98.7% respectively; xylose utilization rate was 84.4%, 84.2% and 86.5% respectively, and cellulose utilization rate was 80.6%, 82.1% and 88.1%, respectively. However, cell growth and sugar utilization were significantly reduced when the ORP was controlled at a more reductive level (less than − 400 mV), suggesting too reductive stress causes toxic effect. Such side effect of reductive stress can also be found in the studies of Wang et al. (2012) and Du et al. (2015). When ORP controlled at -350 mV, butanol reached the maximal production of 10.2 g/L, 34.2% higher than that of the ORP-uncontrolled. Meanwhile, the period of fermentation was shortened from 96 h to 90 h. Ethanol production also increased significantly within the ORP range of -300 ~ -350, from 4.2 g/L for uncontrolled to 5.6 g/L at -300 mV and 5.9 g/L at -350 mV. Compared to the uncontrolled, the maximal of ethanol production was increased by 40.5%. The effect of ORP controlling on butyrate was diametrically opposite to that on butanol and ethanol. ORP at -250 mV presented a slight promotion effect by 19.5% whereas butyrate was inhibited by 11.9%, 16.7%, 35.7% and 45.2% at -275 mV, -300 mV, -350 mV and − 400 mV respectively. ORP controlling also showed inhibition effect on acetate production. The final acetate production decreased from 7.2 g/L (without ORP controlling) to 4.2 g/L at -300mV, 3.9 g/L at -350 mV and 3.1 g/L at -400 mV respectively. The increased solvents/acids ratio under ORP controlling within − 250 mV to -350 mV indicated that the product profiles were shifted to favor solvents over acids production (Du et al., 2015). ORP controlling also inhibits the hydrogen production from 4.5 L of uncontrolled to 3.1 L at -300 mV and 1.7 L at -350 mV (the production profiles of hydrogen and carbon dioxide were given in Appendix D). According to the previous studies conducted by (Du et al., 2015; Xia et al., 2015a), the decreased hydrogen production help to produce additional NADH that favor butanol biosynthesis. Strikingly, the ORP controlling did not affect the carbon dioxide production with a final production about 5.6 L, indicating that the carbon dioxide production is relatively rigid and not easily disturbed by ORP.

3.3 Analysis of the ORP controlling enhancement mechanism on detoxicated SECS fermentability for butanol production

Obviously, the broth ORP enhances fermentability of the detoxicated SECS by affecting the cells' metabolism. To better understand the working mechanism, genome scale metabolic flux analysis (MFA) was performed to compare the flux profiles of *C. acetobutylicum* cells under three different culture conditions: the synthetized medium group (SG), detoxicated SECS medium with ORP control at -350mV (OCG) and without ORP control (UCG). The analysis result was given in Fig. 4.

3.3.1 ORP regulation triggers metabolic flux redistribution in C. acetobutylicum ATCC 824

Figure 4 compared the difference of flux distributions at the typical time point of 36 h (cell growth in acidogenesis phase) and 60h (solventogenesis phase) among the three groups. Figure 4A showed the fitted result of biomass of SG with *Boltzmann* model for the specific growth rate calculation. The other two groups and the detailed calculation process together with the calculation code were given in **Appendix E**. The genome scale metabolic model used in our study consists of 432 genes, 502 reactions and 479 metabolites. Calculation was carried out using FBA constrained by experimental data (Li et al., 2021b). To assess the diversity among the three groups with regards to metabolic flux distribution, principal component analysis (PCA) was carried out (Fig. 4D). We can see that samples from the three groups can be clearly separated, indicating that the metabolic characteristic differences of *C. acetobutylicum* ATCC 824 under different fermentation.

Figure 4B showed the topology structure of the metabolic networks, which only preserves the nodes with significant differences calculated by *p* test lower than 0.05 among the three groups at 36 h. The substrates with the most significant differences are succinyl-CoA (No.62, KEGG: C00091), pyruvate (No.55, KEGG:C00022) and N-Acetyl-L-glutamate 5-semialdehyde (NO. 6, KEGG:C01250). Pyruvate and succinyl-CoA are among the 12 basic biosynthetic precursor

compounds that are used to build macromolecules such as nucleic acids and proteins (Orth, 2012). Their differences may be related to cell growth. N-acetyl-l-glutamate 5-semialdehyde is one of the essential precursors for arginine synthesis (Module ID: M00028 in KEGG database). Previous studies have shown that the synthesis of arginine is an energetically expensive process. The cell has to supply high amounts of ATP for this process. Therefore, N-acetyl-l-glutamate 5-semialdehyde might be closed with the differences in the availability of ATP (Korneli et al., 2012; Xia et al., 2015b). However, it is difficult to determine the potential bottlenecks limiting the production based on such information. Hence, it seems highly important to get further insight into the underpinning metabolism. Since ORP directly affects intracellular electron transfer and redox balance involved in intracellular metabolism. The analysis on NADPH, NADH and ATP was carried out

Figure 4C summarized the major redox reactions in acetone-butanol-ethanol fermentation by the bacterium *Clostridium (*Dai et al., 2021). Figure 4F, Table 3 and Table 4 exhibited the flux distributions among reactions of intracellular force reduction and energy metabolism under the three conditions. In our model, there are 23 reactions involved NADPH, 16 reactions involved NADH and 61 reactions involved ATP. The metabolism of NADPH in the three groups is given in Table 3. At 36h, UCG owned the most active metabolism of NADPH with a total NADPH flux as high as 11.44 mmol/g/h, which is 2.1 and 3.26-fold of SG and OCG. The contributions of each reaction in SG and OCG were similar, except the total flux. In these two groups, respiratory chain was the main source of NADPH, accounting for about 97.7%. Then folate (CA_C2083) and riboflavin synthesis (CA_C0590) account for about 3.09%. However, in the UCG group, the folate synthesis pathway consumed 19.32% of NADPH instead of generation, suggesting the cells in this group consume a large amount of folic acid. This is very reasonable since folic acid is widely involved in the metabolism of cofactors and plays an important role in microbial resistance to stress environment. Compared with 36h, the main source of NADPH at 60h were respiratory chain (EMP19) and TCA cycle (PYR3). Amino acid metabolism (CA_C0510) and carbohydrate metabolism (SULFUR5, CA_C2390) at 60 h tended to decrease. The reaction of fatty acids (CA_C1589, CA_C0764) and COA synthesis (CA_C3254) was significantly enhanced.

Table 3

Simulation of metabolic flux of the NADPH generation/consumption reaction of *C. acetobutylicum* ATCC 824 strain under the different conditions. The unit o mmol/g/h. SG: the synthetized medium group, OCG: detoxicated SECS medium with ORP control at -350mV, UCG: detoxicated SECS medium without ORP cor abbreviations of the reactions were provided in Appendix A.

Reaction	36 h						60 h				
	SG		OGG		UCG		SG		OGG		UCG
	Flux	Percentage	Flux	Percentage	Flux	Percentage	Flux	Percentage	Flux	Percentage	Flux
EMP19	5.28	97.91	3.43	97.82	11.44	99.97	9.30	94.99	7.95	95.68	5.28
AMSU8	-0.03	-0.63	-0.02	-0.55	-0.02	-0.14	0	0	0	0	0
NITROGEN6	-1.95	-36.19	-1.25	-35.83	-3.03	-26.51	0	0	0	0	0
SULFUR5	-0.64	-11.78	-0.45	-12.72	-0.31	-2.70	0	0	0	0	0
GST2	-0.33	-6.09	-0.21	-5.88	-2.42	-21.16	-0.12	-1.26	-0.11	-1.38	-0.08
GST3	-0.23	-4.34	-0.15	-4.20	-2.38	-20.76	-0.05	-0.56	-0.05	-0.61	-0.04
VLI3	-0.07	-1.35	-0.05	-1.40	-0.04	-0.31	-0.04	-0.39	-0.04	-0.43	-0.02
VLI7	-0.28	-5.12	-0.17	-4.83	-0.13	-1.17	-0.15	-1.49	-0.14	-1.63	-0.09
LYS2	-0.09	-1.75	-0.06	-1.65	-0.05	-0.40	-0.05	-0.51	-0.05	-0.56	-0.03
PRO4	-0.08	-1.41	-0.05	-1.33	-0.04	-0.32	0.01	0.12	0.01	0.13	0.01
PTT4	-0.17	-3.18	-0.11	-3.11	-0.08	-0.73	-0.09	-0.93	-0.08	-1.01	-0.06
UREA3	-0.1	-1.82	-0.06	-1.65	-0.05	-0.42	0	0	0	0	0
PYRM16	-0.24	-4.42	-0.16	-4.43	-0.12	-1.01	0	0	0	0	0
PL7	-0.2	-3.76	-0.13	-3.68	-0.10	-0.86	0.10	1.03	0.09	1.12	0.06
FAS3	-0.06	-1.1	-0.04	-1.07	-0.03	-0.25	-0.22	-2.29	-0.21	-2.50	-0.14
FAS4	-0.49	-9.16	-0.32	-9.14	-0.24	-2.10	-0.04	-0.45	-0.04	-0.49	-0.03
FAS5	-0.08	-1.42	-0.05	-1.49	-0.04	-0.33	-0.02	-0.17	-0.02	-0.19	-0.01
FAS6	-0.04	-0.72	-0.03	-0.82	-0.02	-0.17	-0.16	-1.66	-0.15	-1.81	-0.10
FAS7	-0.29	-5.33	-0.20	-5.70	-0.14	-1.22	-0.01	-0.12	-0.01	-0.13	-0.01
PANCOA2	-0.01	-0.17	-0.01	-0.27	0.00	-0.04	0.00	-0.05	0.00	-0.06	0.00
RIBFLA6	0.01	0.14	0.01	0.28	0.00	0.03	0.00	0.04	0.00	0.05	0.00
FOLATE13	-0.01	-0.26	-0.01	-0.26	-0.01	-0.06	0	0	0	0	0
FOLATE18	0.11	1.95	0.07	1.90	-2.21	-19.32	*0.01*	*0.12*	*0.01*	*0.13*	0.01
FOLATE12	0	0	0	0	0	0	*-0.01*	*-0.08*	*-0.01*	*-0.08*	0.00
NITROGEN4	0	0	0	0	0	0	*-0.01*	*-0.14*	*-0.01*	*-0.15*	-0.01
PRO2	0	0	0	0	0	0	*-0.04*	*-0.41*	*-0.04*	*-0.45*	-0.03
PYR3	0	0	0	0	0	0	0.26	2.65	0.24	2.90	0.17

Table 4

Simulation of metabolic flux of the **NADH** generation/consumption reaction of *C. acetobutylicum* ATCC 824 strain under the different conditions. The uni
mmol/g/h. SG :the synthetized medium group, OCG : detoxicated SECS medium with ORP control at -350mV, UCG: detoxicated SECS medium without OR

Reaction	36 h						60 h				
	SG		OGG		UCG		SG		OGG		UCG
	Flux	Percentage	Flux	Percentage	Flux	Percentage	Flux	Percentage	Flux	Percentage	Flux
EMP10	19.01	94.47	12.43	94.81	14.42	78.25	12.35	74.56	9.84	76.88	6.99
EMP18	0.41	2.03	0.45	3.4	2.48	13.44	3.39	20.48	2.63	20.53	1.94
BUTAN1	-0.26	-1.28	-1.03	-8	1.37	7.41	-0.36	-2.19	-0.35	-2.75	-0.3
BUTAN2	-0.22	-1.09	-1.01	-7.81	-0.88	-4.76	-0.35	-2.10	-0.84	-6.53	-0.4
BUTAN6	-4.13	-20.54	-3.11	-24.08	-5.44	-29.55	-3.95	-23.84	-2.83	-22.13	-2.0
BUTAN8	-8.26	-41.08	-6.21	-48.17	-10.89	-59.10	-6.80	-41.03	-4.70	-36.72	-3.5
BUTAN11	-3.52	-17.49	-0.7	-5.44	-0.56	-3.01	-0.55	-3.32	-0.48	-3.78	-0.2
BUTAN12	-3.52	-17.49	-0.7	-5.44	-0.56	-3.01	-0.15	-0.88	-0.63	-4.96	-0.2
TCA2	-0.07	-0.33	-0.04	-0.33	-0.03	-0.17	0.16	0.94	0.00	0.02	0.02
VLI12	0.07	0.36	0.03	0.36	0.03	0.19	0.04	0.23	0.04	0.27	0.02
HIS9	0.02	0.12	0.02	0.12	0.01	0.06	0.01	0.08	0.01	0.09	0.01
HIS10	0.02	0.12	0.02	0.12	0.01	0.06	0.00	0.00	0.00	0.00	0.00
PTT18	0.13	0.66	0.07	0.68	0.06	0.35	0.00	0.00	0.00	0.00	0.00
PUR27	0.03	0.17	0.02	0.17	0.02	0.09	0.15	0.91	0.02	0.15	0.05
PYRM4	0.05	0.26	0.02	0.26	0.03	0.14	0.03	0.17	0.03	0.20	0.02
FOLATE16	-0.14	-0.72	-0.09	-0.73	-0.07	-0.38	0.06	0.34	0.05	0.40	0.04
EMP16	0	0	0	0	0	0	-9.29	-56.09	-7.99	-62.41	-5.4
GST9	0	0	0	0	0	0	0.38	2.28	0.18	1.41	0.18
LIMPIN3	0	0	0	0	0	0	0.00	0.03	0.00	0.03	0.00
PL6	0	0	0	0	0	0	-0.11	-0.65	-0.10	-0.78	-0.0
TCA7	0	0	0	0	0	0	-0.10	-0.58	-0.09	-0.69	-0.0

Table 4 shows the metabolism of NADH in the three groups. At 36h, the NADH fluxes of the three groups were 19.74, 12.66 and 18.43 mmol/g/h respectively. In SG and OCG, the contribution of EMP pathway to NADH was 94%, while that in UCG was only 78.25%. On the contrary, the respiratory chain intensity of the latter group was 6.05 times and 5.51 times that of the first two groups, respectively. It is suggested that the inhibitor decreased the metabolic intensity of EMP. As a compensation mechanism, cells enhanced the metabolic intensity of the respiratory chain. In the UCG, reaction **Butan1 (**acetaldehyde → acetyl coenzyme A) and reaction **Butan8** (acetyl coenzyme A →3-hydroxybutyryl COA) were significantly improved. This change can decrease the synthesis of butyryl COA and ethanol, so as to saving the NADH consumption. At 60H, not surprisingly, SG and OCG owned high flux in almost all the NADH-involved reactions. The total NADH flux of the three groups was 16.57, 12.80 and 9.27 mmol/g/h respectively. This may explain the reason for the high yield of solvents in the first two groups.

Table 5 shows the metabolism of ATP in the three groups. In the genome scale model, there are 61 reactions involved in ATP metabolism, accounting for 12.15% of the total reactions, indicating that ATP metabolism has a very wide impact on cell metabolism. The total ATP flux of the three groups were 44.91, 35.89 and 29.11 mmol/g/h respectively. ATP is mainly used for bacterial synthesis at 36 h, accounting for 42.32% in SG, 42.72% in OCG and 40.16% in UCG of the total ATP respectively (seen **Appendix H**). Compared with UCG, four reactions in OCG has significantly enhanced, which were FOLATE19(CA_C3201/[EC:6.3.4.3])increased by 159 times, GST4 (CA_C1235/ [EC:2.7.1.39]) increased by 116 times, GST1 (CA_C0278/ [EC:2.7.2.4] or CA_C1810/ [EC:2.7.2.4]) increased by 11 times and TCA1 (CA_C2660/ [EC:6.4.1.1]) increased by 6.24 times. FOLATE19□CA_C3201/ [EC:6.3.4.3]) is the synthesis of 10-Formyltetrahydrofolate. This substance is the precursor of many cofactors, suggesting, again, ORP induced high-speed synthesis of cofactors of *C. acetobutyricum.* GST4 and GST1 represent the reactions catalyzed by homoserine kinase [EC:2.7.1.39] and aspartate kinase [EC:2.7.2.4] respectively. They are the key enzymes in aspartate metabolic pathway, which controls the biosynthesis of lysine, methionine, threonine and isoleucine. TCA1 is the reaction catalyzed by pyruvate carboxylase [EC:6.4.1.1]. As the key enzyme of oxaloacetate replenishment pathway in bacteria, it serves as the gate of carbon flow into TCA cycle. In other words, folate, amino acid and TCA cycle of cells were greatly improved under the controlling of oxidoreduction potential. At 60 h the fluxes of four reactions in UCG were at a higher level. it showed 3.23 times higher of PUR17 (CA_C3112/ EC: 2.7.4.3), 1.67 times higher of PANCOA4 (CA_C3200/ [EC:2.7.1.33]), 1.66 times higher of BUTAN10 (CA_C3075/ [EC:2.7.2.7]) and 1.53 times higher of BUTAN4 (CA_C1743/ [EC:2.7.2.1]) of that in OCG. PUR17 [EC: 2.7.4.3] represents the conversion reaction of ATP to ADP, indicating that UCG has higher ADP generation rate. PANCOA4 [EC:2.7.1.33] is a key

enzyme that catalyzes COA synthesis. BUTAN4[EC:2.7.2.1] and BUTAN10[EC:2.7.2.7] are the key enzymes that catalyze butyryl phosphate to butyric acid and butanoyl-COA to butyryl phosphate, respectively. These four key enzymes formed a reaction circuit resulting of acid accumulation. The illustration of the metabolic circuit is given in Fig. 4E. The circuit includes three parts: I）PANCOA4 and PUR17 supply COA and ADP respectively. II) COA and ADP are catalyzed by Butan4 [EC: 2.7.2.1] and butan10 [EC: 2.7.2.7] for butyric acid and acetic acid biosynthesis. III) Under the catalysis of butyryl-CoA-acetoacetate CoA-transferase (EC: 2.8.3.9), acetic acid can capture the CoA group from butanoyl-CoA and convert the latter into butyric acid. The resulted acetoacetyl-CoA can further convert into butyric acid in this circuit. Wang et al. (2011) and Maddox et al. (2000) studied the cause of *"acid crash"* by adding acid to the culture medium. For the first time, we found a new metabolism circuit that may cause butyric acid accumulation by metabolic pathway analysis method.

3.3.2 ORP regulation changes intercellular redox status

Metabolic flux reflects the instantaneous change in cell metabolism. In order to further confirm the real state of cells, we measured the key metabolites, including ATP concentration, NADH/NAD^+ and NADPH/$NADP^+$, within *C. acetobutylicum* ATCC 824 from the three groups during the solvent-producing phase. As shown in Fig. 5a, all the factors measured in SG kept the highest level among the three groups, followed by those in OCG. Taking the time point of 60 h as example (when the butanol biosynthesis rate was the highest at this point), the ATP concentration in SG is 1.2-fold and 1.5-fold of that in OCG and UCG, respectively; the NADH/NAD + ratio in SG is 2.2-fold of that in OCG and 4.0-fold of that in UCG; and the NADPH/$NADP^+$ ratio in SG is 1.4-fold of that in OCG and 2.3-fold of that in UCG correspondingly. High energy and reducing power availability form one of the main reasons for high butanol production in SG and OCG. Meanwhile, we also detected the activities of key enzymes in the butanol biosynthesis and the result was shown in Fig. 5b. The high activities of butyraldehyde and butanol dehydrogenase in SG explained its high butanol production in the fermentation. Comparing with the ORP uncontrolled group, the activities of butyraldehyde and butanol dehydrogenase in OCG were increased by 2.1-fold and 1.2-fold. Meanwhile, the phosphotransbutyrylase activity was decreased by 29%, indicating that ORP controlling shift more butyryl-CoA towards butanol biosynthesis at the expense of butyrate. It is interesting to note that phosphotransbutyrylase in UCG kept at a stable level, suggesting butyrate was produced continuously during the whole process. This result is quite consistent with our above analysis

3.3.3 ORP regulation changes cell membrane integrity

A major drawback of solvent production by microorganisms is the toxic effect of the alcohols, especially n-butanol, on the cells themselves (Alsaker et al., 2010). It is well known that *n*-butanol influences the lipid composition, fluidity, and the potential of the membrane and is able to interrupt the phospholipid bilayer of the cell. This toxic effect severely limits the butanol production, even causing cell autolysis (Janssen et al., 2012). Therefore, the ability of cells to withstand the accumulation of toxic products without loss of productivity is a most significant goal (Tomas et al., 2004). Studies showed that the cell's resistance ability depends on a unique mechanism, namely *homeoviscous adaptation*, which is that *clostridia* increases saturated fatty acid chain content to modulate their membrane fluidity in the presence of solvents (Alsaker et al., 2010). As key factors for fatty acid and amino acids biosynthesis (Akashi & Gojobori, 2002; Alsaker et al., 2010; Xia et al., 2015a; Xia et al., 2013), it is reasonable to presume that the enhanced ATP, NDPH and NADH availability by ORP controlling can improve the tolerance ability of *C. acetobutylicum* ATCC 824. To verify our prediction, cell membrane integrity in the three groups were compared and the result was given in Fig. 6.

Fluorescein diacetate (FDA) is a cell-permeant esterase substrate. As Fig. 5a shown, when absorbed, it can be converted into green fluorescent compound "*fluorescin*" by esterase in the living cell, which can be detected by measuring the fluorescence or absorbance of the sample (Clarke et al., 2001). When the cell membrane was damaged and the permeability increased, FAD will leak from the cell, insulting the decrease of fluorescence intensity. Therefore, it can be used to judge the cell membrane integrity by the change of fluorescence intensity (Chand et al., 1994). In the comparison experiments, butanol was supplemented into the three groups (SG, OCG, and UCG) to keep at a final concentration of 20 g/L and samples were withdrawn very 2 h for cell membrane detection. The result was given in Fig. 6.

We can see that the fluorescence intensity dropped quickly during the first 6 h, with a percentage of 35.1% in SG, 61.7% in OCG and 77.3% in UCG, suggesting there exists differences on the cell membrane integrity among the three groups. Comparing with UCG, the cell membrane integrity was increased by 15.6% in OCG. It also can be found that the decrease of fluorescence intensity trended smaller with processing time increased, especially after 6 h, indicating cell had trigger *homeoviscous adaptation* to resistant the toxic effect of butanol. Therefore, by experiment, we obtain direct evidence that ORP controlling can increased the cell membrane integrity of *C. acetobutylicum*. It contributed to the enhancement of butanol production under ORP controlling.

4. Conclusions

This paper applied the ORP controlling strategy to enhance the butanol production with enzymatically hydrolyzed steam-exploded corn stover (SECS). At the optimal ORP level, solvent and butanol production reached 18.1 g/L and 10.2 g/L, an 27.5% and 34.2% increase compared with the ORP uncontrolled group, respectively. In-depth analysis showed three issues resulted in significant improvement in cell growth and butanol production: First, Glycolysis and TCA circulation pathway are strengthened through key nodes such as pyruvate carboxylase [EC: 6.4.1.1], which provides sufficient NADH and NADPH for the cell. Second, sufficient ATP is provided to avoid "*acid crash*". Third, the key enzymes activities regulating butanol biosynthesis and cell membrane integrity was improved.

Declarations

Ethics approval and consent to participate

This article does not contain any studies involving human or animal participants.

Consent for publication

Not applicable.

Availability of data and materials

All data generated or analyzed in this study are included in the published article.

Competing interests

The authors declare that they have no competing interests.

Funding

This work was financially supported by Tianjin Municipal Education Commission (2017KJ009).

Authors' contributions

MW and MLX conceived and designed the experiments and contributed reagents/materials. MLX, DW, and YMX performed the experiments. MLX, DW, YMX, HJS, and ZYT contributed to the writing of the manuscript. YZ and MW supervised the research and edited the manuscript. All authors read and approved the final manuscript.

Acknowledgements

The authors would like to thank the members of the Industrial Fermentation Microbiology Laboratory in the Tianjin University of Science & Technology for their valuable comments and helpful discussions.

Author information

State Key Laboratory of Food Nutrition and Safety. Key Laboratory of Industrial Fermentation Microbiology, Ministry of Education. College of Biotechnology, Tianjin University of Science & Technology, Tianjin 300457, People's Republic of China

References

1. Akashi H, Gojobori T: **Metabolic efficiency and amino acid composition in the proteomes of *Escherichia coli* and *Bacillus subtilis*.** *Proc Natl Acad Sci U S A* 2002, 99(6):3695-3700.
2. Alsaker KV, Paredes C, Papoutsakis ET: **Metabolite stress and tolerance in the production of biofuels and chemicals: gene-expression-based systems analysis of butanol, butyrate, and acetate stresses in the anaerobe *Clostridium acetobutylicum*.** *Biotechnol Bioeng* 2010, 105(6):1131-1147.
3. Baral NR, Shah A: **Microbial inhibitors: formation and effects on acetone-butanol-ethanol fermentation of lignocellulosic biomass.** *Appl Microbiol Biotechnol* 2014, 98(22):9151-9172.
4. Bowles LK, Ellefson WL: **Effects of butanol on *Clostridium acetobutylicum*.** *Appl Environ Microbiol* 1985, 50(5):1165-1170.
5. Chand S, Lusunzi I, Veal DA, Williams LR, Karuso P: **Rapid screening of the antimicrobial activity of extracts and natural products.** *J Antibiot (Tokyo)* 1994, 47(11):1295-1304.
6. Chen H, Qiu W: **Key technologies for bioethanol production from lignocellulose.** *Biotechnol Adv* 2010, 28(5):556-562.
7. Cheng K, Martin-Sancho L, Pal LR, Pu Y, Riva L, Yin X, Sinha S, Nair NU, Chanda SK, Ruppin E. **Genome-scale metabolic modeling reveals SARS-CoV-2-induced metabolic changes and antiviral targets.** *Mol Syst Biol* 2021, 17(11):e10260.
8. Clarke JM, Gillings MR, Altavilla N, Beattie AJ: P**otential problems with fluorescein diacetate assays of cell viability when testing natural products for antimicrobial activity.** *J Microbiol Methods* 2001, 46(3):261-267.
9. Dai Z, Zhu Y, Dong H, Zhao C, Zhang Y, Li Y: **Enforcing ATP hydrolysis enhanced anaerobic glycolysis and promoted solvent production in *Clostridium acetobutylicum*.** *Microb Cell Fact* 2021, 20(1):149.
10. Du Y, Jiang W, Yu M, Tang IC, Yang ST: **Metabolic process engineering of *Clostridium tyrobutyricum* Δack-adhE2 for enhanced n-butanol production from glucose: effects of methyl viologen on NADH availability, flux distribution, and fermentation kinetics.** *Biotechnol Bioeng* 2015, 112(4):705-715.
11. Ezeji T, Milne C, Price ND, Blaschek HP: **Achievements and perspectives to overcome the poor solvent resistance in acetone and butanol-producing microorganisms.** *Appl Microbiol Biotechnol* 2010, 85(6):1697-1712.
12. Ezeji T, Qureshi N, Blaschek HP: **Butanol production from agricultural residues: Impact of degradation products on *Clostridium beijerinckii* growth and butanol fermentation.** *Biotechnol Bioeng* 2007, 97(6):1460-1469.

13. Heipieper HJ, Weber FJ, Sikkema J, Keweloh H, de Bont, J.A: **Mechanisms of resistance of whole cells to toxic organic solvents.** *Trends Biotechnol* 1994, 12(10), 409-415.
14. Heirendt L, Arreckx S, Pfau T, Mendoza SN, Richelle A, Heinken A, Haraldsdóttir HS, Wachowiak J, Keating SM, Vlasov V, Magnusdóttir S, Ng CY, Preciat G, Žagare A, Chan SHJ, Aurich MK, Clancy CM, Modamio J, Sauls JT, Noronha A, Bordbar A, Cousins B, El Assal DC, Valcarcel LV, Apaolaza I, Ghaderi S, Ahookhosh M, Ben Guebila M, Kostromins A, Sompairac N, Le HM, Ma D, Sun Y, Wang L, Yurkovich JT, Oliveira MAP, Vuong PT, El Assal LP, Kuperstein I, Zinovyev A, Hinton HS, Bryant WA, Aragón Artacho FJ, Planes FJ, Stalidzans E, Maass A, Vempala S, Hucka M, Saunders MA, Maranas CD, Lewis NE, Sauter T, Palsson BØ, Thiele I, Fleming RMT: **Creation and analysis of biochemical constraint-based models using the COBRA Toolbox v.3.0.** *Nat Protoc* 2019, 14(3):639-702.
15. Himmel ME, Ding SY, Johnson DK, Adney WS, Nimlos MR, Brady JW, Foust TD: **Biomass recalcitrance: engineering plants and enzymes for biofuels production.** *Science* 2007, 9;315(5813):804-7.
16. Ibraheem O, Ndimba BK: **Molecular adaptation mechanisms employed by ethanologenic bacteria in response to lignocellulose-derived inhibitory compounds.** *Int J Biol Sci* 2013, 28;9(6):598-612.
17. Janssen H, Grimmler C, Ehrenreich A, Bahl H, Fischer RJ: **A transcriptional study of acidogenic chemostat cells of *Clostridium acetobutylicum*–solvent stress caused by a transient n-butanol pulse.** *J Biotechnol* 2012, 31;161(3):354-65.
18. Korneli C, Bolten CJ, Godard T, Franco-Lara E, Wittmann C: **Debottlenecking recombinant protein production in *Bacillus megaterium* under large-scale conditions–targeted precursor feeding designed from metabolomics.** *Biotechnol Bioeng* 2012, 109(6):1538-50.
19. Lee J, Yun H, Feist AM, Palsson BØ, Lee SY: **Genome-scale reconstruction and in silico analysis of the *Clostridium acetobutylicum ATCC 824* metabolic network.** *Appl Microbiol Biotechnol* 2008, 80(5):849-62.
20. Li S, Ye Z, Moreb EA, Hennigan JN, Castellanos DB, Yang T, Lynch MD: **Dynamic control over feedback regulatory mechanisms improves NADPH flux and xylitol biosynthesis in engineered *E. coli*.** *Metab Eng* 2021, 64:26-40.
21. Li X, Li ZG, Shi ZP: **Metabolic flux and transcriptional analysis elucidate higher butanol/acetone ratio feature in ABE extractive fermentation by *Clostridium acetobutylicum* using cassava substrate.** *Bioresour Bioprocess* 2014, 1(1), 1-13.
22. Li Y, Sun H, Wang Y, Yang S, Wang J, Wu T, Lu X, Chu Y, Chen F: **Integrated metabolic tools reveal carbon alternative in *Isochrysis zhangjiangensis* for fucoxanthin improvement.** *Bioresour Technol* 2022, 347:126401.
23. Liu CG, Xue C, Lin YH, Bai FW: **Redox potential control and applications in microaerobic and anaerobic fermentations.** *Biotechnol Adv* 2013, 31(2):257-65.
24. Liu XB, Gu QY, Yu XB: **Repetitive domestication to enhance butanol tolerance and production in *Clostridium acetobutylicum* through artificial simulation of bio-evolution.** *Bioresour Technol* 2013, 130:638-43.
25. Maddox IS, Steiner E, Hirsch S, Wessner S, Gutierrez NA, Gapes JR, Schuster KC: **The cause of "acid-crash" and "acidogenic fermentations" during the batch acetone-butanol-ethanol (ABE-) fermentation process.** *J Mol Microbiol Biotechnol* 2000, 2(1):95-100.
26. Mussatto SI, Roberto IC: **Chemical characterization and liberation of pentose sugars from brewer's spent grain.** *J Chem Technol Biot* 2006, 81(3), 268-274.
27. Nagarajan H, Sahin M, Nogales J, Latif H, Lovley DR, Ebrahim A, Zengler K: **Characterizing acetogenic metabolism using a genome-scale metabolic reconstruction of *Clostridium ljungdahlii*.** *Microb Cell Fact* 2013, 25;12:118.
28. Orth, Jeffrey David: **Systems biology analysis of *Escherichia coli* for discovery and metabolic engineering**. *Dissertations & Theses – Gradworks* University of California, San Diego, 2012.
29. Rodenburg SYA, Seidl MF, de Ridder D, Govers F: **Uncovering the Role of Metabolism in Oomycete-Host Interactions Using Genome-Scale Metabolic Models.** *Front Microbiol* 2021, 11;12:748178.
30. Tomas CA, Beamish J, Papoutsakis ET: **Transcriptional analysis of butanol stress and tolerance in *Clostridium acetobutylicum*.** *J Bacteriol* 2004, 186(7):2006-18.
31. Vasconcelos I, Girbal L, Soucaille P: **Regulation of carbon and electron flow in *Clostridium acetobutylicum* grown in chemostat culture at neutral pH on mixtures of glucose and glycerol.** *J Bacteriol* 1994, 176(5):1443-50.
32. Wang L, Chen H: **Increased fermentability of enzymatically hydrolyzed steam-exploded corn stover for butanol production by removal of fermentation inhibitors.** *Process Biochem* 2011, 46(2), 604-607.
33. Wang S, Zhang Y, Dong H, Mao S, Zhu Y, Wang R, Luan G, Li Y: **Formic acid triggers the "Acid Crash" of acetone-butanol-ethanol fermentation by *Clostridium acetobutylicum*.** *Appl Environ Microbiol* 2011, 77(5):1674-80.
34. Wang S, Zhu Y, Zhang Y, Li Y: **Controlling the oxidoreduction potential of the culture of *Clostridium acetobutylicum* leads to an earlier initiation of solventogenesis, thus increasing solvent productivity.** *Appl Microbiol Biotechnol* 2012, 93(3):1021-30.
35. Xia ML, Wang L, Yang ZX, Chen HZ: **Periodic-peristole agitation for process enhancement of butanol fermentation.** *Biotechnol Biofuels* 2015, 23;8:225.
36. Xia M, Huang D, Li S, Wen J, Jia X, Chen Y: **Enhanced FK506 production in *Streptomyces tsukubaensis* by rational feeding strategies based on comparative metabolic profiling analysis.** *Biotechnol Bioeng* 2013, 110(10):2717-30.
37. Xia M, Peng M, Xue D, Cheng Y, Li C, Wang D, Lu K, Zheng Y, Xia T, Song J, Wang M: **Development of optimal steam explosion pretreatment and highly effective cell factory for bioconversion of grain vinegar residue to butanol.** *Biotechnol Biofuels* 2020, 24;13:111.
38. Xia ML, Wang L, Yang ZX, Chen HZ: **Periodic-peristole agitation for process enhancement of butanol fermentation**. *Biotechnol Biofuels* 2015, 23;8:225.
39. Zheng Y, Yuan Q, Yang X, Ma H. **Engineering *Escherichia coli* for poly-(3-hydroxybutyrate) production guided by genome-scale metabolic network analysis.** *Enzyme Microb Technol* 2017, 106:60-66.
40. Zhu HF, Liu ZY, Zhou X, Yi JH, Lun ZM, Wang SN, Tang WZ, Li FL: **Energy Conservation and Carbon Flux Distribution During Fermentation of CO or H_2/CO_2 by *Clostridium ljungdahlii*.** *Front Microbiol* 2020, 17;11:416.

Figures

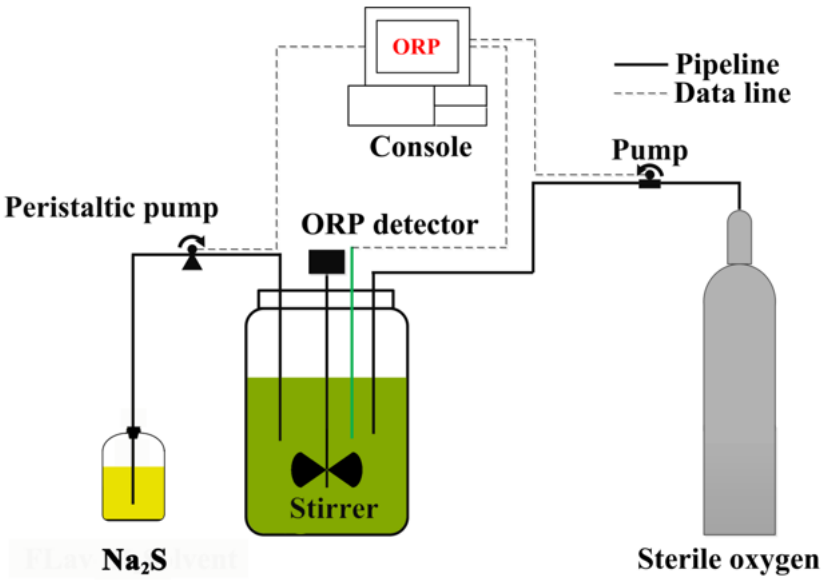

Figure 1

Legend not included with this version

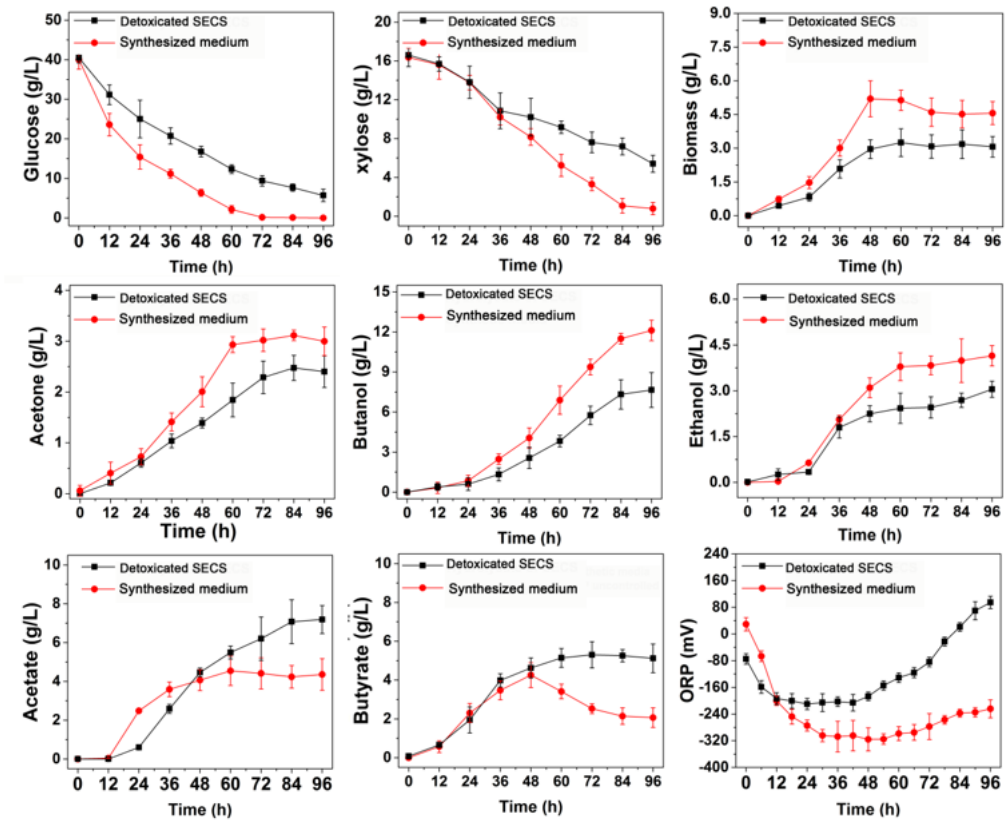

Figure 2

Legend not included with this version

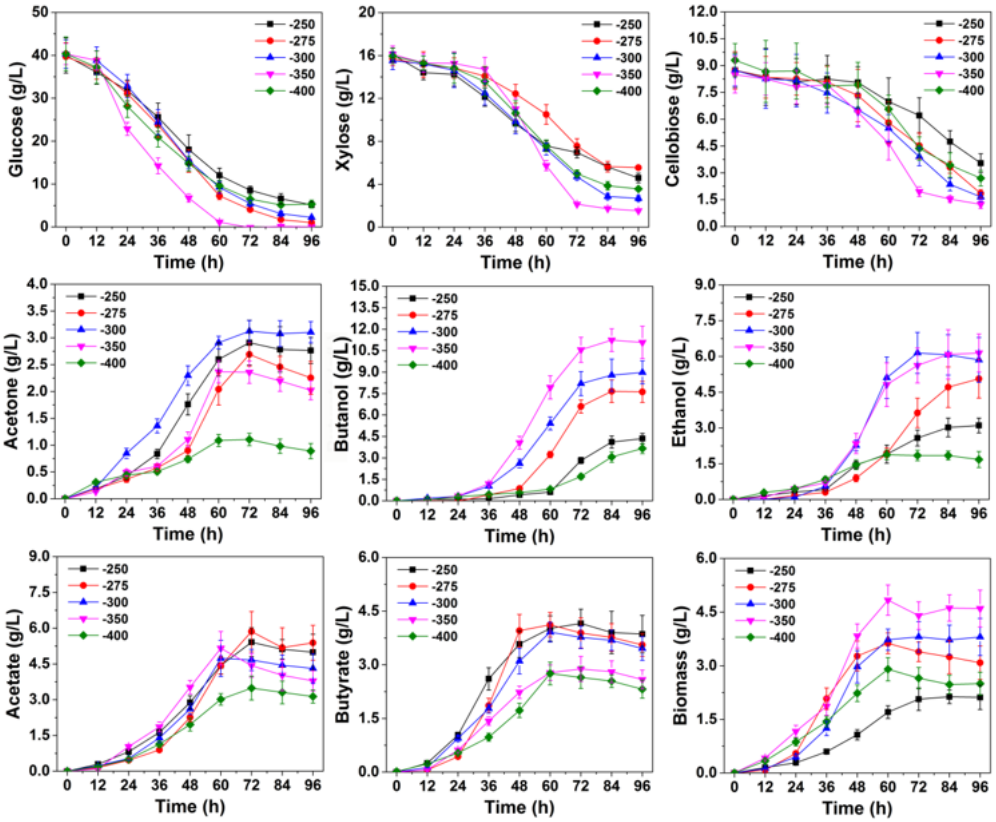

Figure 3

Legend not included with this version

Figure 4

Legend not included with this version

Figure 5

Legend not included with this version

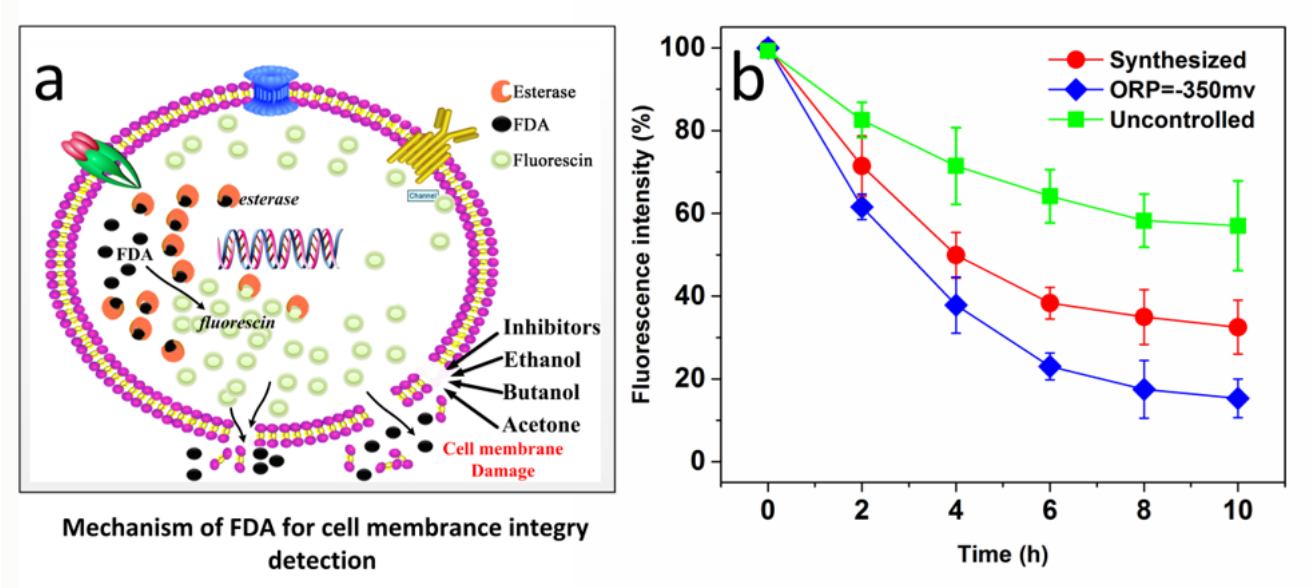

Figure 6

Legend not included with this version

Supplementary Files

This is a list of supplementary files associated with this preprint. Click to download.

- AppendixA.pdf
- AppendixB.docx
- AppendixC.docx
- AppendixD.docx
- AppendixE.docx
- AppendixF.xlsx
- AppendixG.xlsx
- AppendixH.xlsx